Supporting Information for

Observation and Reanalysis Derived Relationships Between Cloud and Land Surface Fluxes Across Cumulus and Stratiform Coupling Over the Southern Great Plains

Tianning Su[1,2]*, Zhanqing Li[1]*, Yunyan Zhang[2], Youtong Zheng[3], Haipeng Zhang[1]

[1]Department of Atmospheric and Oceanic Sciences & ESSIC, University of Maryland, College Park, Maryland 20740, USA

[2]Lawrence Livermore National Laboratory, Livermore, CA, USA

[3]Department of Atmospheric and Earth Science, University of Houston, Houston, TX, USA

*Corresponding authors: zhanqing@umd.edu; su10@llnl.gov

Contents of this file

This PDF file includes:

Text S1
Figs. S1 to S9

S. 1 Descriptions of datasets:

(1) Thermodynamic profiles from radiosonde

We will use radiosonde measurements to characterize the thermodynamic settings of the PBL. Radiosondes are routinely launched multiple times at the ARM sites. Holdridge et al. (2011) provided technical details about the ARM radiosonde. Using the well-established method developed by Liu and Liang (2010), we retrieved PBLHs over the SGP site based on the vertical profiles of potential temperature from radiosonde measurements.

(2) Active Remote Sensing of Clouds (ARSCL)

We will use the well-established ARM cloud product, named ARSCL, generated for each ARM site (Clothiaux et al., 2000). ARSCL provides the vertical boundaries of clouds by combining data from the MPL, ceilometer, and cloud radar, conveying useful information pertaining to the vertical structure and temporal evolution of clouds (Kollias et al., 2007). For the lowest cloud base, we will use the best estimation from laser-based techniques (i.e., MPL and ceilometer). Based on ARSCL, Xie et al. (2010) offers a comprehensive dataset of cloud fraction profiles.

(3) Surface fluxes

Surface fluxes are critical for PBL development and closely interact with low clouds as the driving force. A value-added product at ARM called the bulk aerodynamic latent and sensible heat fluxes from energy balance Bowen ratio (BAEBBR) was generated to replace energy balance Bowen ratio flux measurements with a bulk aerodynamic estimation when the Bowen Ratio (Wesely et al., 1995). We use the Best Estimate Sensible/Latent Heat Fluxes in the BAEBBR product.

(4) ARMBE2DGRID

The ARMBE2DGRID VAP provides a dataset by integrating key surface measurements from the Southern Great Plains sites, consolidating them into a uniform

2D grid (https://www.arm.gov/capabilities/science-data-products/vaps/armbe2dgrid). The dataset delivers hourly data with a spatial resolution of 0.25° x 0.25°. It encompasses a wide range of products including Surface Meteorological Instrumentation, data from Oklahoma Mesonet and Kansas State University Mesonet, Quality Controlled Radiation Data, observations from Geostationary Operational Environmental Satellites, Microwave Radiometer, Best-Estimate Fluxes from BAEBBR, ECOR outputs, and Soil Water and Temperature System data. Rigorous Quality Controls are employed to ensure the reliability of the data.

(5) MODIS aboard the NASA Aqua and Terra

NASA's Aqua and Terra satellites, carrying the Moderate Resolution Imaging Spectroradiometer (MODIS), provides high-quality data on global cloud coverage. The corrected reflectance product from MODIS offers a true-color view of the Earth's surface and atmosphere, allowing for accurate confirmation of cloud presence and extent (Schaaf et al., 2002). By analyzing the true-color imagery, we can inspect cloud regimes, checking stratiform and cumulus for coupled clouds. NASA MODIS imageries are achieved in https://worldview.earthdata.nasa.gov/.

(6) ERA-5 Reanalysis Data

As one of the most advanced and widely used reanalysis data, ERA-5, produced by the European Centre for Medium-Range Weather Forecasts (ECMWF), provides a high-resolution, hourly updated global atmospheric reconstruction (Hersbach et al. 2020). Utilizing advanced assimilation of vast amounts of observational data, ERA-5 offers comprehensive climate variables, including temperature, humidity, wind, and cloud properties. We used this dataset to compare cloud-land relationships between observation and reanalysis datasets. With its fine spatial resolution and temporal coverage, ERA-5 allows for analysis of cloud formation, relating to PBL thermodynamics and surface processes.

(7) MERRA-2 Reanalysis Data

The Modern-Era Retrospective analysis for Research and Applications, Version 2 (MERRA-2), developed by NASA, is an improved reanalysis dataset focusing on the representation of the hydrological cycle, aerosols, and atmospheric composition (Gelaro et al., 2017). MERRA-2 integrates satellite and ground-based observational data to provide a coherent record of the global atmosphere. The low cloud fraction data are provided at a temporal resolution of one hour, while the vertical cloud fraction are available at three-hour intervals. In this study, MERRA-2's extensive coverage and detailed depiction of atmospheric variables are used to examine the cloud occurrences and their relationship with surface fluxes.

Figures

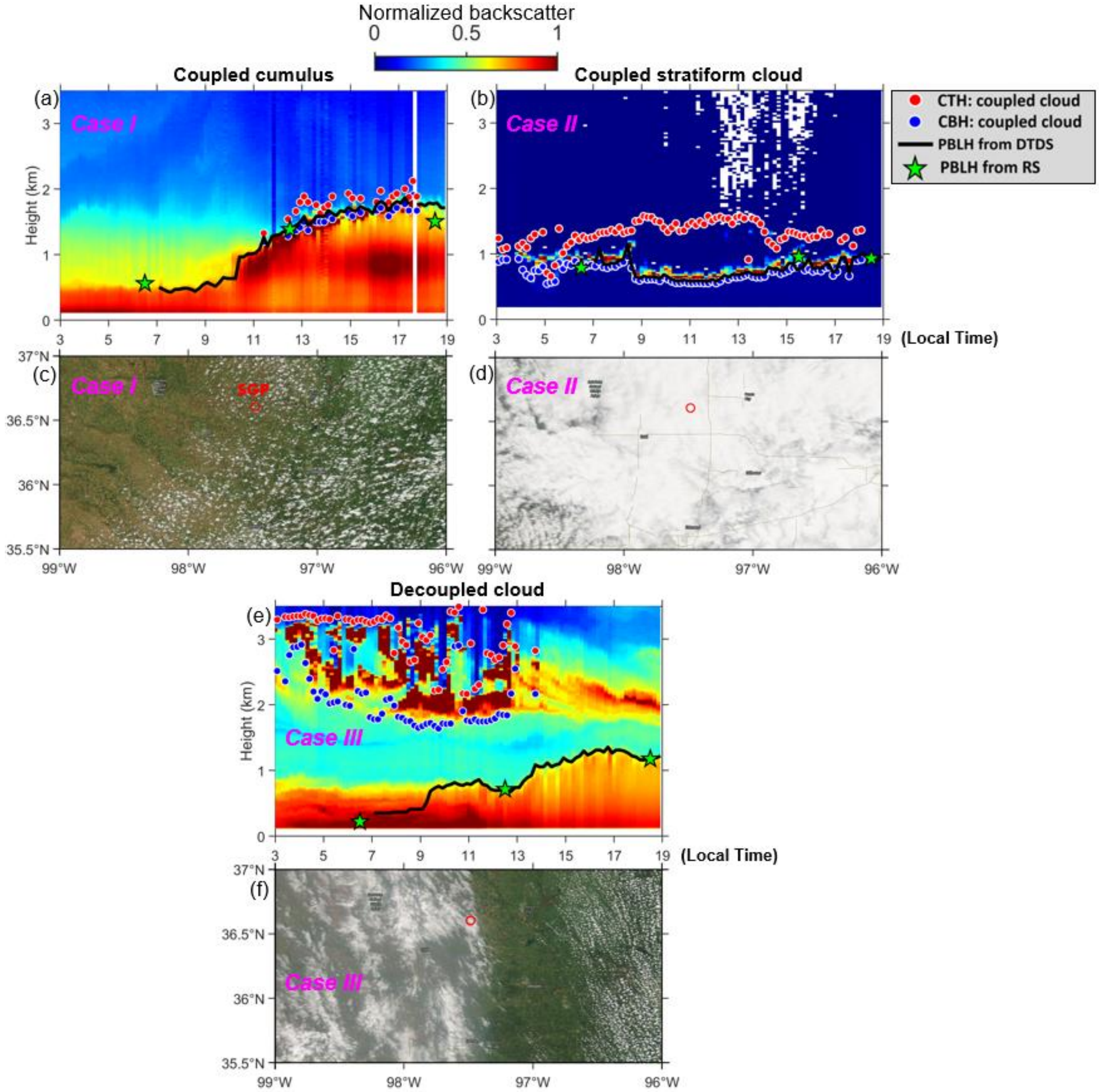

Figure S1. Daily vertical profiles of backscatters for coupled cumulus (a, Case I) and coupled stratiform cloud (b, Case II). Backscatter is normalized to a range of 0-1, in arbitrary units. Red dots and blue dots indicate the CTH and CBH of coupled cloud. Black lines and green stars mark the PBLH retrieved from MPL and radiosonde. (c and d) 2-D view of the corrected reflectance (true color) derived from MODIS (Aqua) for Case I (c) and Case II (d). The red circle marks the position of SGP site. (e-f) Daily vertical profiles of backscatters and the satellite image for decoupled cloud (Case III).

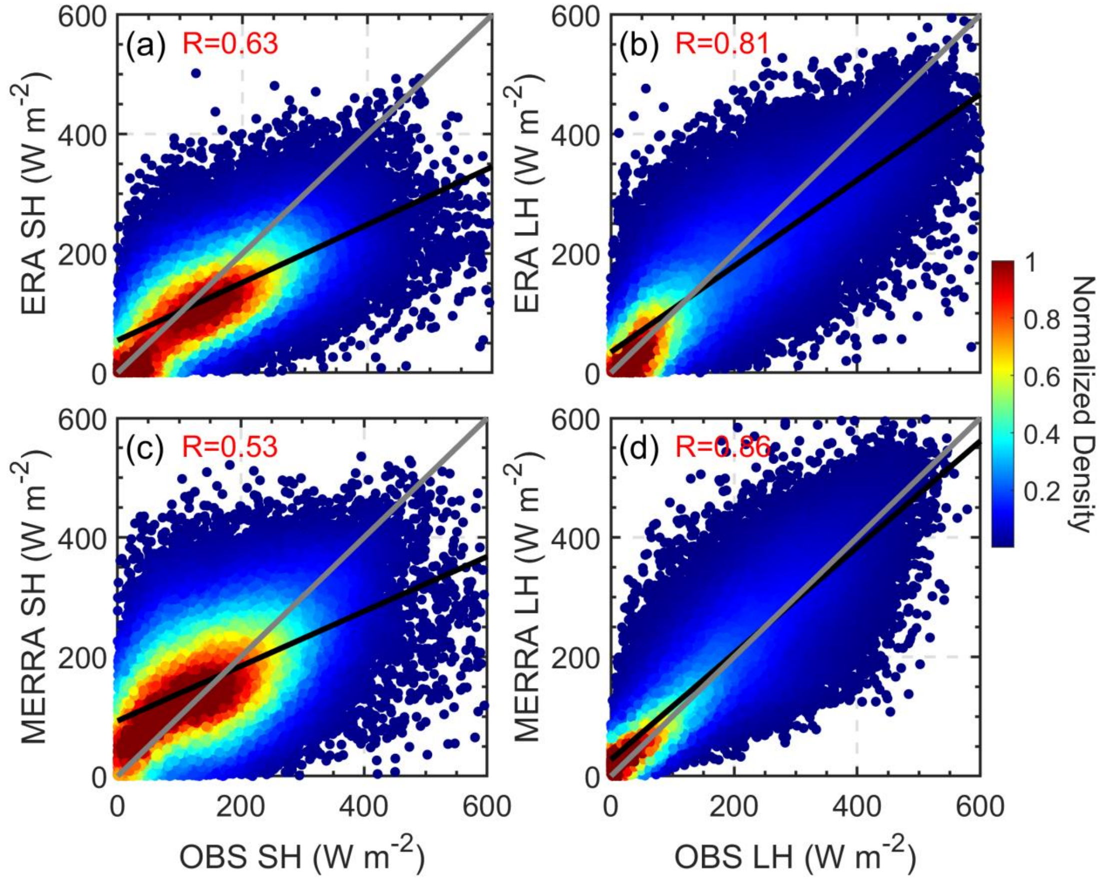

Figure S2. Density scatterplots of the comparison between observed surface fluxes and reanalysis surface fluxes during 09:00-15:00 Local Time (OBS SH: observed sensible heat; OB LH: observed latent heat; ERA SH: sensible heat from ERA-5; ERA LH: latent heat from ERA-5; MERRA SH: sensible heat from MERRA-2; MERRA LH: latent heat from MERRA-2). The correlation coefficients (R) are given in each panel. The solid black lines represent the linear regression, and the dashed grey lines denote 1:1 line.

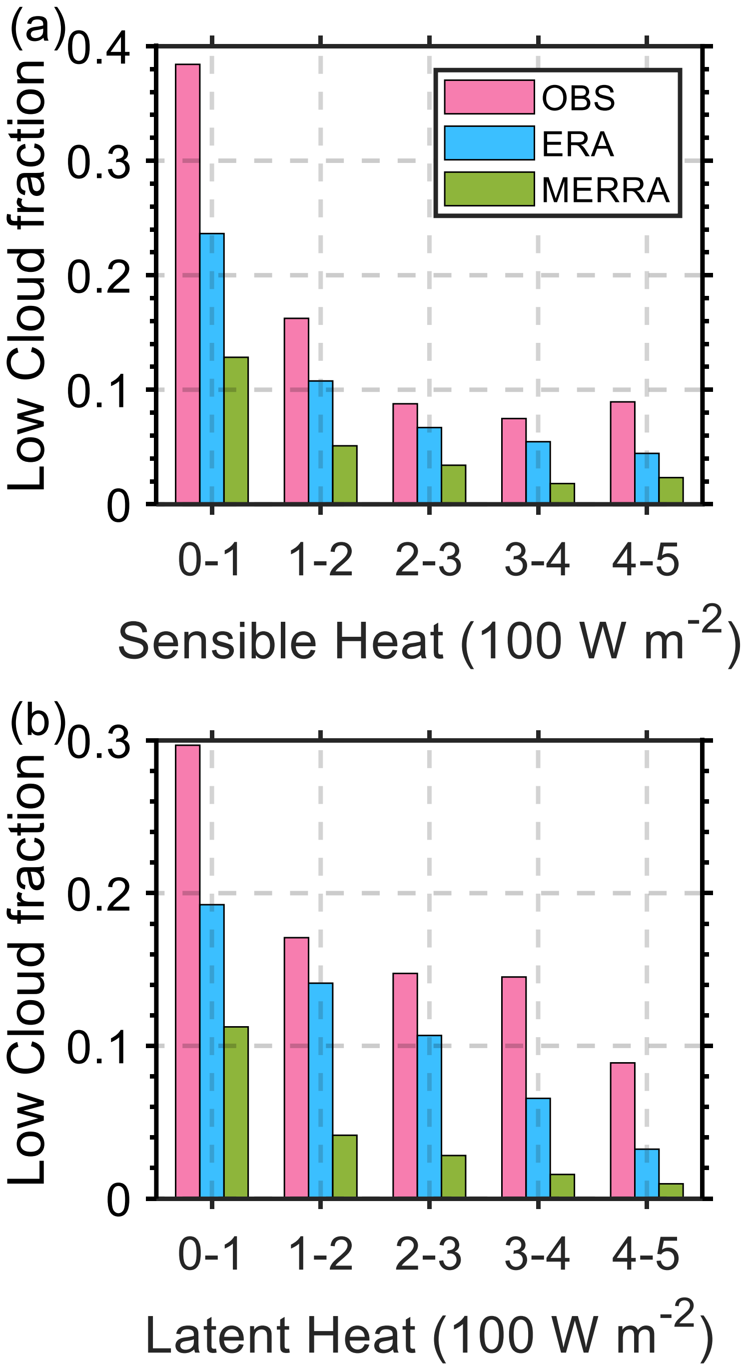

Figure S3. Comparison of average low cloud fraction across varying ranges of sensible and latent heat fluxes. The low cloud fraction is defined as the maximum cloud fraction occurring between the surface and 700 hPa. The data are categorized by source, with observations (OBS), ERA-5, and MERRA-2 depicted in pink, blue, and green bars, respectively.

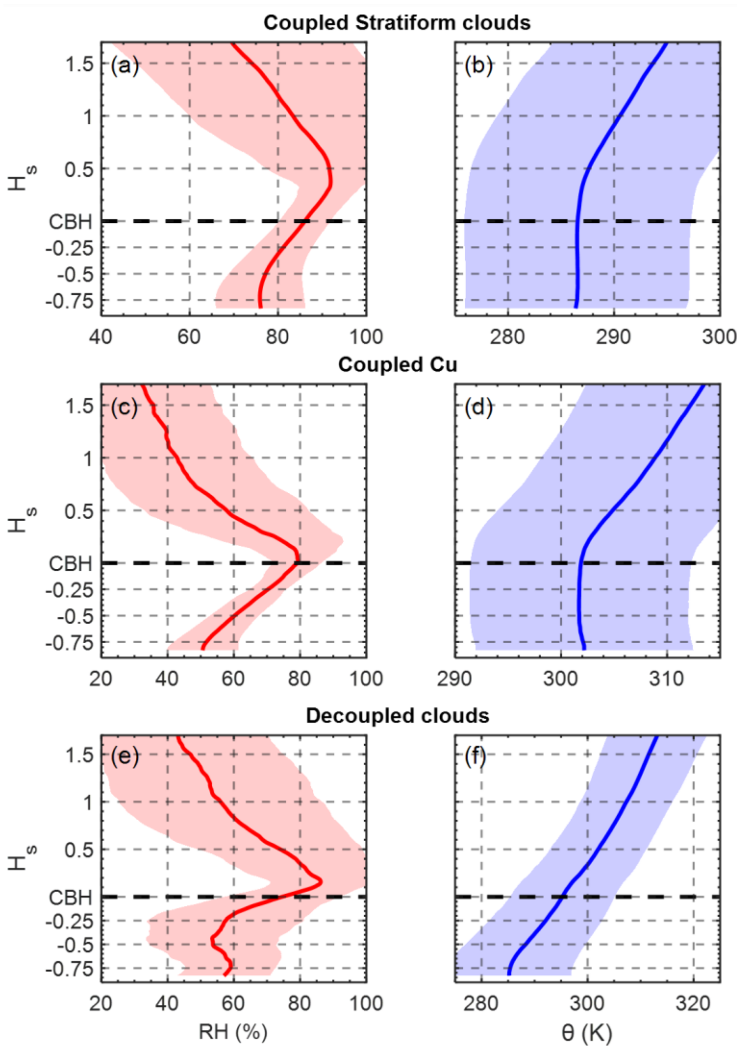

Figure S4. The average profiles of RH (red line) and virtual potential temperature (θ_v, blue line) for (a) coupled stratiform cloud, (b) coupled cumulus, and (c) decoupled cloud. The vertical scale is normalized by CBH (black dash line). The red and blue shaded areas indicate the standard deviations for RH and virtual potential temperature, respectively.

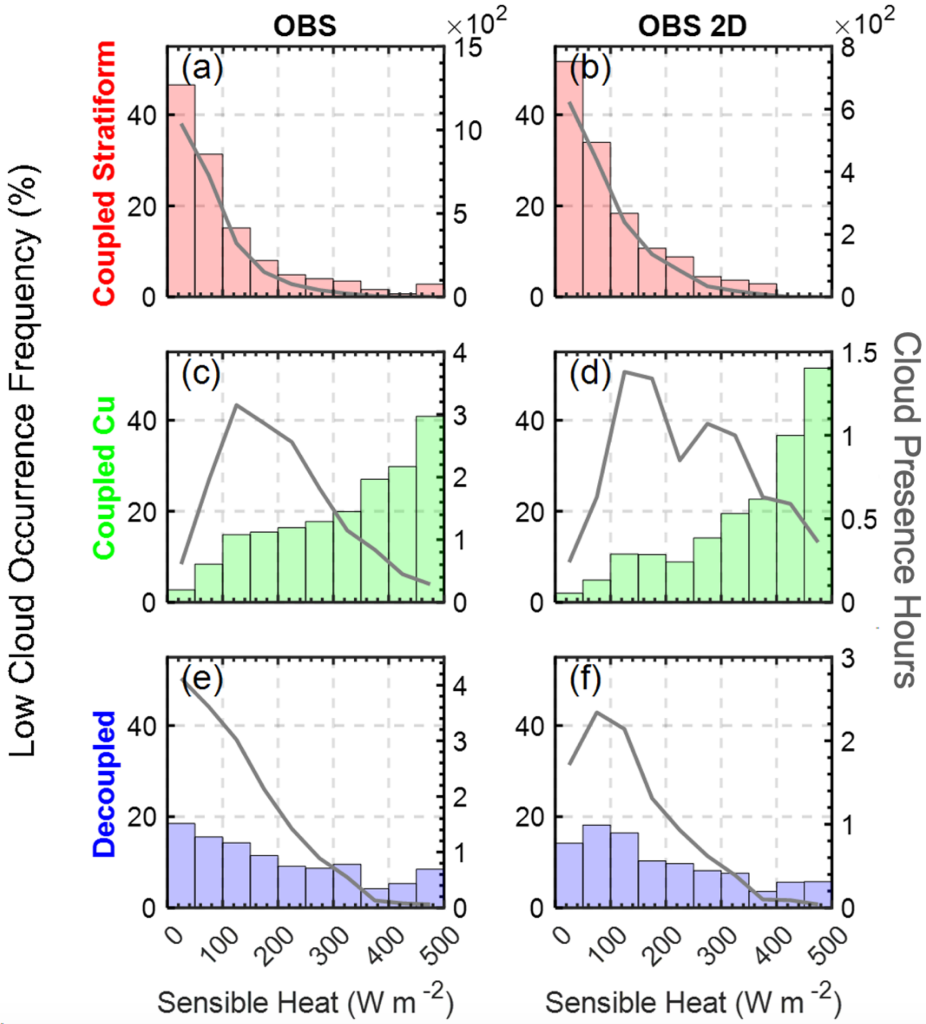

Figure S5. Cloud occurrence frequency and surface sensible heat relationships segregated by conditions of cloud regimes during 09:00-15:00 LT. The histograms display the average frequency of different cloud types binned by surface sensible heat flux for point observation (OBS) from the BAEBBR and for the 2D observation (OBS 2D) from the ARMBE2DGRID. Grey lines indicate the number of hours with low cloud occurrence within each flux bin.

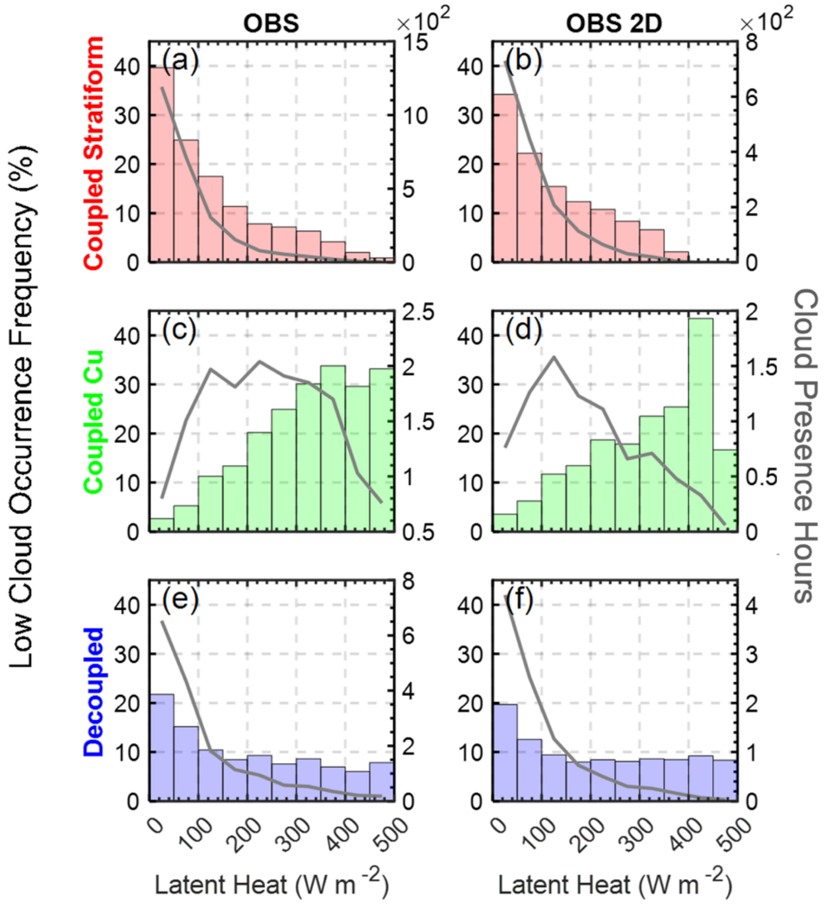

Figure S6. Similar to Figure S5, but depicting the relationships between low cloud occurrence frequency and surface latent heat fluxes.

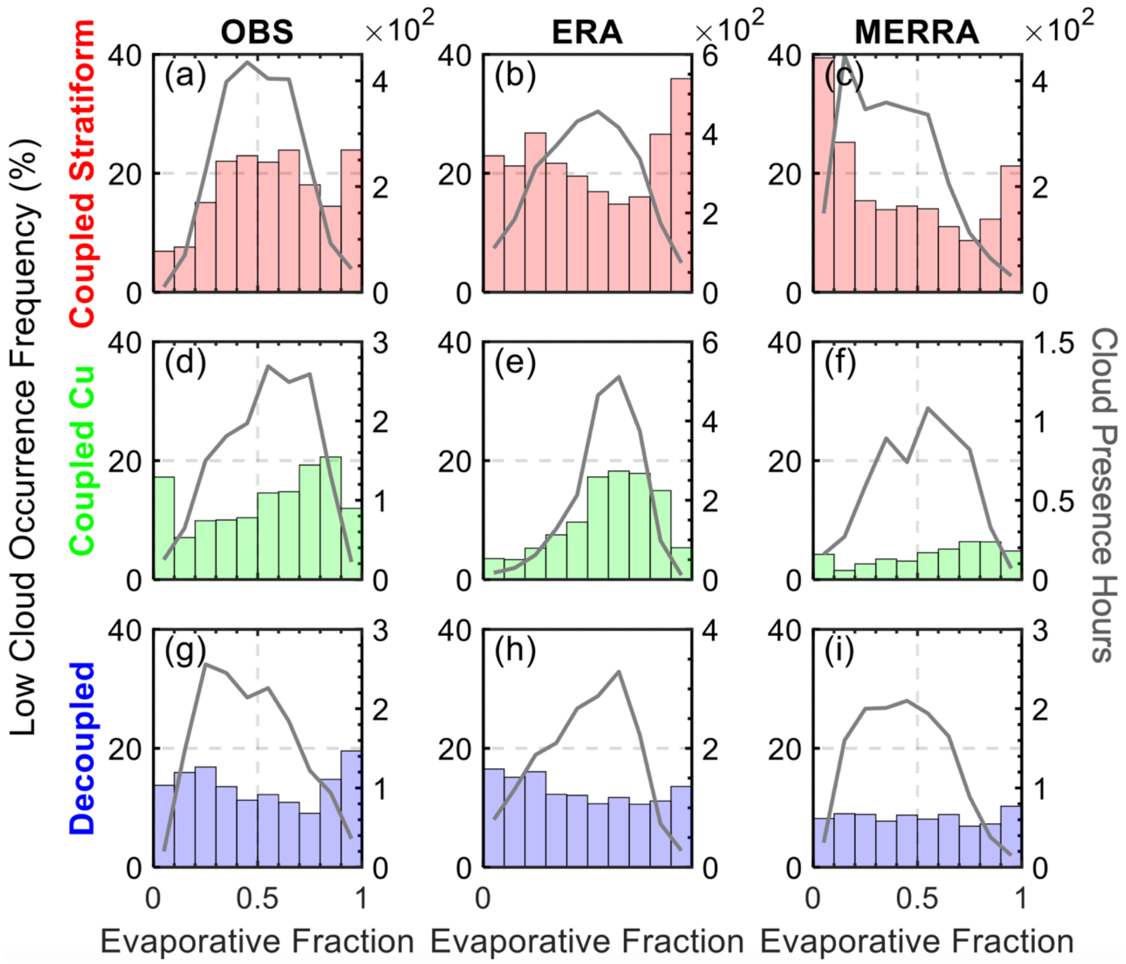

Figure S7. Similar to Figure S5, but depicting the relationships between low cloud occurrence frequency and evaporative fraction. Evaporative fraction is calculated as $\frac{Latent\ Heat}{Latent\ Heat+Sensible\ Heat}$.

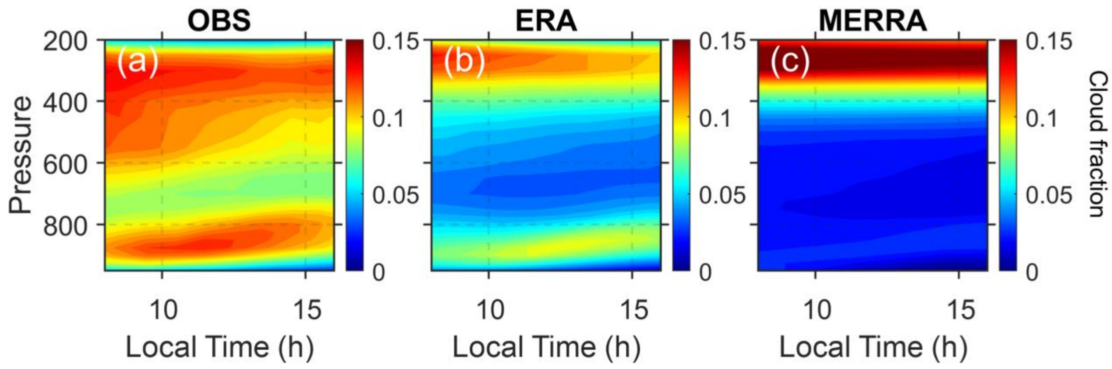

Figure S8. Diurnal Variation of Cloud Fraction in Observations and Reanalysis Data. Contour plots represent the diurnal cycle of cloud fraction as a function of pressure (in hPa) for observational (OBS, a) and two reanalysis datasets (ERA and MERRA, b-c).

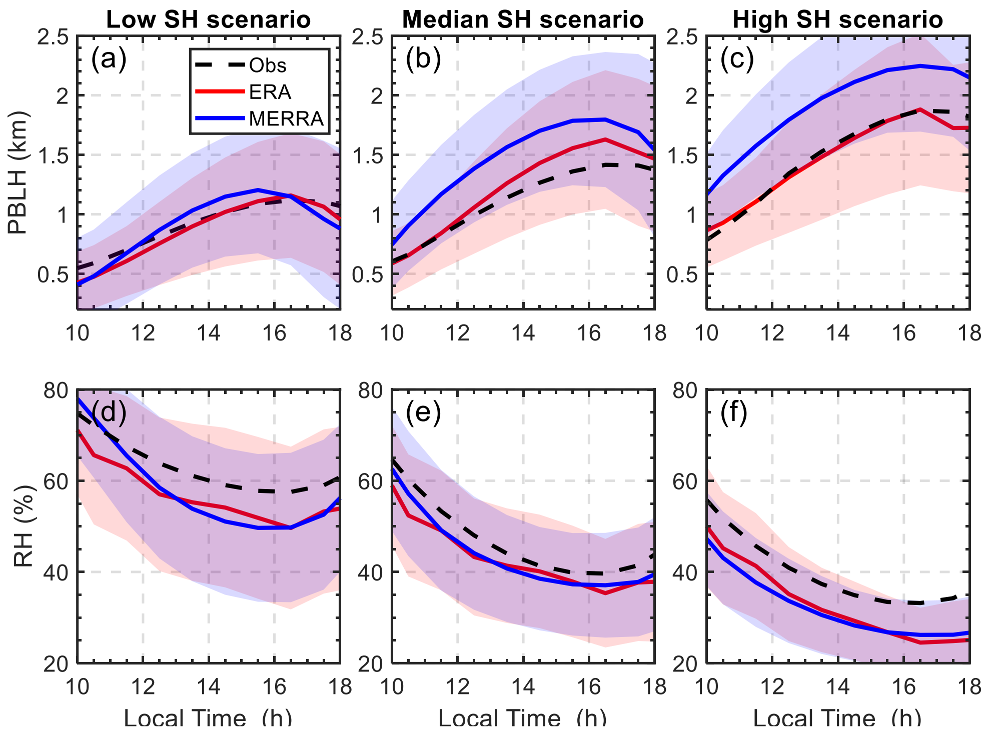

Figure S9. Diurnal variations in PBLH and RH across different sensible heat (SH) scenarios. The graphs illustrate the progression of PBLH and RH throughout the day, segmented into three sensible heat categories: low (0-200) (a, d), median (200-400) (b, e), and high (>400 W m^{-2}) (c, f). Solid lines represent the mean values from observations (Obs), ERA-5 reanalysis (ERA), and MERRA-2 reanalysis (MERRA). Shaded areas indicate one standard deviation from the mean, providing a visual representation of variability within each dataset.

References

Clothiaux, E. E., Ackerman, T. P., Mace, G. G., Moran, K. P., Marchand, R. T., Miller, M. A., & Martner, B. E. (2000). Objective determination of cloud heights and radar reflectivities using a combination of active remote sensors at the ARM CART sites. Journal of Applied Meteorology, 39(5), 645-665.

Gelaro, R., McCarty, W., Suárez, M.J., Todling, R., Molod, A., Takacs, L., Randles, C.A., Darmenov, A., Bosilovich, M.G., Reichle, R. and Wargan, K., 2017. The modern-era retrospective analysis for research and applications, version 2 (MERRA-2). Journal of climate, 30(14), pp.5419-5454.

Hersbach, H., Bell, B., Berrisford, P., Hirahara, S., Horányi, A., Muñoz-Sabater, J., Nicolas, J., Peubey, C., Radu, R., Schepers, D. and Simmons, A., 2020. The ERA5 global reanalysis. Quarterly Journal of the Royal Meteorological Society, 146(730), pp.1999-2049.

Holdridge, D., Ritsche, M., Prell, J., and Coulter, R. (2011): Balloon-borne sounding system (SONDE) handbook, https://www.arm.gov/capabilities/instruments/sonde.

Liu, S., & Liang, X. Z. (2010). Observed diurnal cycle climatology of planetary boundary layer height. Journal of Climate, 23(21), 5790-5809.

Schaaf, C.B., Gao, F., Strahler, A.H., Lucht, W., Li, X., Tsang, T., Strugnell, N.C., Zhang, X., Jin, Y., Muller, J.P. and Lewis, P., 2002. First operational BRDF, albedo nadir reflectance products from MODIS. Remote sensing of Environment, 83(1-2), pp.135-148.

Wesely, M. L., Cook, D. R., and Coulter, R. L. (1995): Surface heat flux data from energy balance Bowen ratio systems (No. ANL/ER/CP-84065; CONF-9503104-2). Argonne National Lab., IL (United States).

Xie, S., McCoy, R.B., Klein, S.A., Cederwall, R.T., Wiscombe, W.J., Clothiaux, E.E., Gaustad, K.L., Golaz, J.C., Hall, S.D., Jensen, M.P. and Johnson, K.L., 2010. Clouds and more: ARM climate modeling best estimate data: A new data product for climate studies. Bulletin of the American Meteorological Society, 91(LLNL-JRNL-412676).